The American Journal of Pathology, Vol. 175, No. 5, November 2009

DOI: 10.2353/ajpath.2009.090210

Molecular Pathogenesis of Genetic and Inherited Diseases

Altered Chondrocyte Differentiation and Extracellular Matrix Homeostasis in a Zebrafish Model for Mucolipidosis II

Heather Flanagan-Steet, Christina Sias, and Richard Steet

From the Complex Carbohydrate Research Center, University of Georgia, Athens, Georgia

Mucolipidosis II (ML-II) is a pediatric disorder caused by defects in the biosynthesis of mannose 6-phosphate, the carbohydrate recognition signal responsible for targeting certain acid hydrolases to lysosomes. The mechanisms underlying the developmental defects of ML-II are largely unknown due in part to the lack of suitable animal models. To overcome these limitations, we developed a model for ML-II in zebrafish by inhibiting the expression of *N*-acetylglucosamine-1-phosphotransferase, the enzyme that initiates mannose 6-phosphate biosynthesis. Morphant embryos manifest craniofacial defects, impaired motility, and abnormal otolith and pectoral fin development. Decreased mannose phosphorylation of several lysosomal glycosidases was observed in morphant lysates, consistent with the reduction in phosphotransferase activity. Investigation of the craniofacial defects in the morphants uncovered striking changes in the timing and localization of both type II collagen and Sox9 expression, suggestive of an accelerated chondrocyte differentiation program. Accumulation of type II collagen was also noted within misshapen cartilage elements at later stages of development. Furthermore, we observed abnormal matrix formation and calcium deposition in morphant otoliths. Collectively, these data provide new insight into the developmental pathology of ML-II and suggest that altered production and/or homeostasis of extracellular matrix proteins are integral to the disease process. These findings highlight the potential of the zebrafish system in studying lysosomal disease pathogenesis. ***(Am J Pathol 2009, 175:2063–2075; DOI: 10.2353/ajpath.2009.090210)***

Proper catabolism of macromolecules within the lysosome is necessary to maintain the normal function of cells and their surrounding environment. The importance of this process in human health is underscored by a growing number of genetic diseases that involve defects in the proteins and enzymes responsible for this task. These diseases (termed lysosomal storage disorders or LSDs) have a diverse etiology, encompassing defects in individual acid hydrolases, metabolite transporters, and enzymes that aid in targeting hydrolases to this organelle.[1] Collectively, LSDs are one of the most frequently occurring genetic diseases affecting children in the Unites States, with an estimated incidence of 1 in every 5000 to 7000 live births.

Mucolipidosis II (ML-II or I-cell disease) is an autosomal recessive LSD caused by defects in the enzyme, UDP-GlcNAc:lysosomal enzyme *N*-acetylglucosamine-1-phosphotransferase. This enzyme (herein abbreviated as "phosphotransferase") catalyzes the first step in the biosynthesis of mannose 6-phosphate (M6P) residues on the oligosaccharide chains of most soluble lysosomal hydrolases.[2,3] This recognition marker mediates the binding of lysosomal hydrolases to high-affinity M6P receptors in the trans-Golgi network and their subsequent targeting to the endosomal/lysosomal system via clathrin-coated vesicles.[4] Loss of the M6P recognition marker leads to missorting of newly synthesized lysosomal hydrolases into the extracellular space. On a cellular level, ML-II tissues, particularly those of mesenchymal origin, are characterized by the presence of numerous cytoplasmic inclusions and/or dense lysosomes filled with undigested macromolecules.

The phosphotransferase enzyme exists as a heterohexameric complex composed of three different subunits ($\alpha 2$, $\beta 2$, and $\gamma 2$). The α and β subunits, encoded by a single gene (*GNPTAB*), contain the catalytic activity of the enzyme and also mediate the selective binding of lysosomal enzymes to the enzyme.[5–8] The γ subunit,

Supported by grants from the National Institutes of Health (1 R01 GM86524-01), the Mallinckrodt Foundation, and the University of Georgia Research Foundation.

Accepted for publication July 23, 2009.

Address reprint requests to Richard Steet, Ph.D., Assistant Professor, University of Georgia, Complex Carbohydrate Research Center, 315 Riverbend Rd., Athens, GA 30602. E-mail: rsteet@ccrc.uga.edu.

encoded by a separate gene (*GNPTG*), is thought to modulate the activity of the α/β subunits by an undetermined mechanism.[9,10] Deletions and frameshift mutations in the *GNPTAB* gene that result in little or no residual enzyme activity lead to ML-II (or ML-II α/β), whereas activity-compromising point mutations in this gene cause a milder form of the disease termed ML-IIIA (or ML-III α/β).[11–15]

ML-II is often considered the most severe LSD, with developmental defects that are apparent at or shortly after birth and a highly progressive course. Children with ML-II rarely survive beyond early childhood. The multisystemic clinical presentation of ML-II includes a spectrum of skeletal abnormalities (termed dysostosis multiplex), developmental delay, recurrent lung infections, and heart and craniofacial defects.[16] Like many LSDs, the cellular and molecular pathogenesis of ML-II is poorly defined but may involve mechanisms that extend beyond the lysosomal compartment.[17] Indeed, radiographical and microscopic examination of postmortem human ML-II bone and cartilage has suggested that impaired organization and structure of the extracellular matrix (ECM) are associated with the pathological changes in these tissues.[18,19] The mechanisms whereby loss of M6P biosynthesis leads to impaired maintenance of the extracellular environment of these tissues are unclear.

Understanding the molecular pathogenesis of ML-II is a high priority from a clinical standpoint because there are currently no therapies available for this debilitating disease. Efforts to define the disease process of ML-II have been hampered by the lack of animal models that are both genetically accessible and amenable to the study of early development. The latter of these issues is of particular importance since many of the features of ML-II appear to be because of abnormal fetal development.[20] A feline model for ML-II has been reported that displays pathological and biochemical features consistent with the human condition, including facial dysmorpia, skeletal defects, and faulty targeting of hydrolases to the lysosome.[21–23] This model is limited by the fact that early developmental processes cannot be followed in these animals due to intrauterine gestation. Kornfeld and colleagues[24,25] have also characterized a *GNPTAB* knockout mouse, which exhibits retinal degeneration, reduced size, and pathological lesions in several exocrine glands. Although chondrocytes from these mice were found to be hypertrophic and often distended, fibrocytes and mesenchymal cells did not develop the cytoplasmic vacuolar inclusions characteristically observed in human ML-II and ML-III patients.

In an effort to gain insight into the developmental impact of impaired M6P biosynthesis, we applied a morpholino (MO)-based knockdown strategy to develop phosphotransferase-deficient zebrafish and characterized these morphant embryos using a combination of cellular and molecular approaches. Morphant embryos exhibit multiple phenotypes, including abnormal craniofacial development, impaired motility, and defects in otic vesicle structure. Our detailed investigation of the cartilage defects in the morphants uncovered striking changes in the timing and localization of both type II collagen and Sox9 expression in craniofacial elements, suggestive of an altered chondrocyte differentiation program. Alterations in the homeostasis of the ECM were also noted in the otoliths of the ML-II morphants. Taken together, these findings suggest that impaired production and/or homeostasis of ECM proteins may represent a common pathological mechanism of this disease.

Materials and Methods

Fish Strains, Maintenance, and Breeding

Wild-type zebrafish were obtained from Fish 2U (Gibsonton, FL) and maintained using standard protocols. Embryos were staged according to the criteria established by Kimmel.[26] In some cases, 0.003% 1-phenyl-2-thiourea was added to the growth medium to block pigmentation. All MO-generated phenotypes were tested in several genetic backgrounds, including a wild-type strain from a commercial source (Fish 2U). Analyses of craniofacial phenotypes were performed in both the F2U wild-type strain and Tg (*fli1*:EGFP)^{y1} transgenic line.[27]

Antisense MO Injections

The protein and nucleotide sequences of the zebrafish *N*-acetylglucosamine-1-phosphotransferase α/β subunit (*GNTPAB*) were identified by basic local alignment search tool analysis of the human sequence. Translation-blocking (5′-TTAACGACCAACATGACTCCGGCC-3′) and splice-blocking (5′-TAAACATTTGTAGAGCCAACCTGGT-3′) antisense MOs were designed to the 5′-untranslated region and exon-intron junction between exons 9 and 10, respectively (Gene Tools, Eugene, OR). On the basis of phenotypic and biochemical analyses of various concentrations, 8.2 ng of both MOs was injected into the yolks of one- to two-cell stage embryos. These concentrations were chosen following careful assessment of percent knockdown via enzymatic assays and phenotypic penetrance.

GNTPAB *Cloning and mRNA Rescue*

The full-length coding region of *GNPTAB* was synthetically generated according to the GenBank deposited sequences CAI11844 (Gene Art AG, Toronto, ON, Canada). The cDNA was subsequently cloned into a pCSDest expression vector (provided by Dr. Nathan Lawson, University of Massachusetts Medical School, Worcester, MA). Full-length mRNA was generated with the Message Machine SP6 kit (Roche Scientific, Indianapolis, IN). Rescue experiments were performed on one-cell stage embryos by sequential injections of 8 ng of the splice blocking MO and 50 pg of purified *GNPTAB* mRNA.

GlcNAc-1-Phosphotransferase Enzymatic Activity Assay

Activity of GlcNAc-1-phosphotransferase was measured in microsomal preparations from wild-type and morphant

embryos following MO injection as described previously.[13] Reactions using α-methylmannoside as the acceptor and [^{32}P]UDP-GlcNAc as a substrate were conducted for 90 minutes, and activity units are calculated as pmoles of GlcNAc-[^{32}P] transferred/hour/mg protein.

M6P Receptor Affinity Column

Wild-type and morphant embryo extracts were fractionated using an M6P receptor affinity column as described previously.[8] Activity of lysosomal enzymes was measured in each column fraction using fluorescent substrates: 4-methylumbelliferyl galactoside (for β-galactosidase activity), 4-methylumbelliferyl glucuronide (for β-glucuronidase activity), and 4-methylumbelliferyl β-*N*-acetylglucosaminide (for β-hexosaminidase activity). Reactions were performed in 50 mmol/L citrate buffer (pH 4.5) and 0.5% Triton X-100 containing 3 mmol/L of the respective substrates. The percentage of bound activity relative to total activity recovered from three independent experiments is shown.

Histochemistry and Whole-Mount in Situ *Analysis*

Embryos were stained with Alcian blue as described previously.[28] Bone development was assessed in embryos using a method optimized for dual Alcian blue and Alizarin red staining.[29] Morphometric measurements were performed using the Olympus FV1000 software. Analysis of proliferation by 5-bromo-2′-deoxyuridine (BrdU) labeling was performed according to the protocol outlined by Harris et al.[30] Whole-mount *in situ* analysis was performed as described previously.[31] The plasmids for the sox9a and sox9b probes were provided by Dr. J. Postlethwait (University of Oregon, Eugene, OR).

Whole-Mount Immunohistochemistry

Embryos were stained with the appropriate primary antibodies as described earlier.[32] Antibodies were as follows: anti-BrdU (1/100; Developmental Studies Hybridoma Bank); anti-collagen type II (1/100; Developmental Studies Hybridoma Bank); anti-phospho Smad 2 (1/100; Upstate Cell Signaling, Lake Placid, NY); and anti-sox9 (1/100; Santa Cruz Biotechnology, Santa Cruz, CA). Embryos were imaged on an Olympus FV-1000 laser scanning microscope. Confocal images were acquired as described previously.[32]

Flow Cytometry and FACS Analysis

Wild-type and morphant *fli1*:EGFP embryos were collected in Ca^{2+}-free Ringers solution. Embryonic yolks were removed by passage through a flame polished Pasteur pipette. Embryos were subsequently rinsed for 15 minutes in Ca^{2+}-free Ringer's solution. Dissociated-cellular suspensions were generated by soaking the embryos in 0.25% trypsin, followed by repeated passage through 23- and 25-gauge syringes. Cellular dissociation was monitored microscopically. When cellular aggregates were no longer visible, the suspensions were filtered through sterile 40-μm Falcon filters to remove debris. Cells were collected following centrifugation and suspended in L-15 growth medium (minus phenol red) containing 10% FBS and 10% fish embryo extract. Green fluorescent protein (GFP)-positive and -negative cells were subsequently isolated by flow cytometry.

Results

Depletion of N-*Acetylglucosamine-1-Phosphotransferase Activity in Zebrafish Results in Multiple Developmental Defects*

To assess the developmental impact of impaired M6P biosynthesis, we inhibited the expression of the phosphotransferase enzyme (the *GNPTAB* gene product) in developing zebrafish embryos. Injection of one-cell stage embryos with either translation-blocking or splice-blocking antisense MOs targeting the α/β subunit of GlcNAc-1-phosphotransferase enzyme resulted in multiple phenotypes (Figure 1). At 24 hours postfertilization (hpf), MO-injected embryos (herein referred to as morphants) displayed reduced motility but were otherwise outwardly normal. However, by 48 hpf, morphants began to exhibit a pericardial edema (Figure 1B, red arrows) that subsequently increased in severity, as well as small misshapen eyes and irregular otoliths. In particular, loss of phosphotransferase activity consistently reduced the size and number of ear stones. By 3 days postfertilization (dpf), morphant embryos were significantly affected. They had blunt, rounded neurocraniums, significant heart edema, abnormal otic vesicles, and a pronounced motility defect. In addition, phosphotransferase morphant animals were shorter (10 ± 3%) than their wild-type clutch mates and were often missing one or both pectoral fins (Figure 1E, black arrows). They also lacked swim bladders and consistently displayed reduced yolk consumption, as evidenced by the presence of large irregular yolks at 5 dpf (Figure 1). All of the phosphotransferase morphants died within the first 5 or 6 days of development.

To gauge the level of residual phosphotransferase activity following MO injection, we performed enzymatic assays on detergent extracts from wild-type and MO-injected embryos. In wild-type embryos, phosphotransferase activity was present at relatively steady levels during the first 5 days of development (35 to 51 pmol/mg/hour). Furthermore, *in situ* hybridization experiments showed that *GNPTAB* mRNA was ubiquitously expressed throughout the embryo during the first 5 days of development (data not shown). As shown in Table 1, injection of embryos with various concentrations of MO resulted in a dose-dependent reduction of phosphotransferase activity, with a maximal inhibition of 89% occurring at 4 dpf. Analysis of animals injected with increasing concentrations of MO demonstrated that the penetrance of the phenotypes directly correlated with the degree to which phosphotransferase activity was reduced. Conversely,

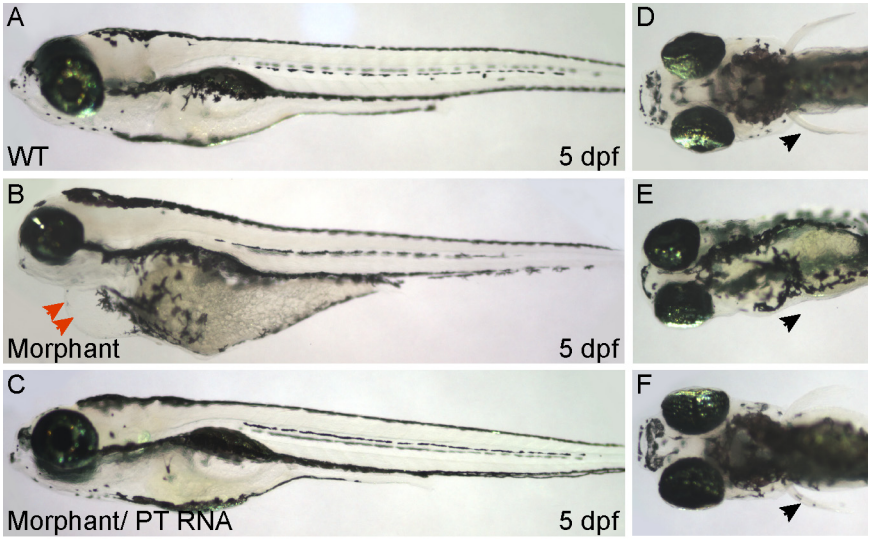

Figure 1. Knockdown of phosphotransferase enzyme results in multiple phenotypes that mirror the developmental defects seen in human ML-II patients. Compared with wild-type (WT) embryos at 5 days postfertilization (**A** and **D**), embryos injected with phosphotransferase MO (**B** and **E**) had rounded neurocraniums and protracted jaws, enlarged hearts, pericardial edema (**B**, **red arrows**), and underused yolks and lacked pectoral fins (**E**, **arrow**). Introduction of wild-type phosphotransferase (PT) mRNA in the morphant background fully rescued each of these phenotypes (**C** and **F**). **Black arrows** denote the position (or lack of) of pectoral fins (**D–F**).

embryos in which phosphotransferase activity had only been reduced by 58% were largely normal and generally indistinguishable from wild-type embryos (Table 1). To determine the half-life of the MO, we measured activity as a function of time in morphant embryos. The maximal effect of highest MO concentrations was observed at 4 dpf, with activity recovering slightly (~10%) by 5 dpf.

Morphant Phenotypes Are Due to Specific Loss of Phosphotransferase Activity

We performed several control experiments to verify that the observed phenotypes were due to specific loss of phosphotransferase activity. First, injection of a 4-bp mismatch MO yielded embryos with no observable phenotypes and did not affect the enzymatic activity of the phosphotransferase (Table 1). Second, to address whether nonspecific apoptotic events contributed to the MO-based phenotypes, embryos were co-injected with the translation blocking phosphotransferase MO and a MO directed against the apoptotic inducer, p53. Concurrent knockdown of p53 has been shown to ameliorate the cellular death induced by off target MO effects.[33] Co-injection of these two MOs resulted in animals that were indistinguishable from animals injected with the translation blocking MO alone. The lack of a significant apoptotic response in MO-injected embryos was confirmed by both TUNEL analyses and acridine orange stains of wild-type and phosphotransferase morphant embryos (data not shown).

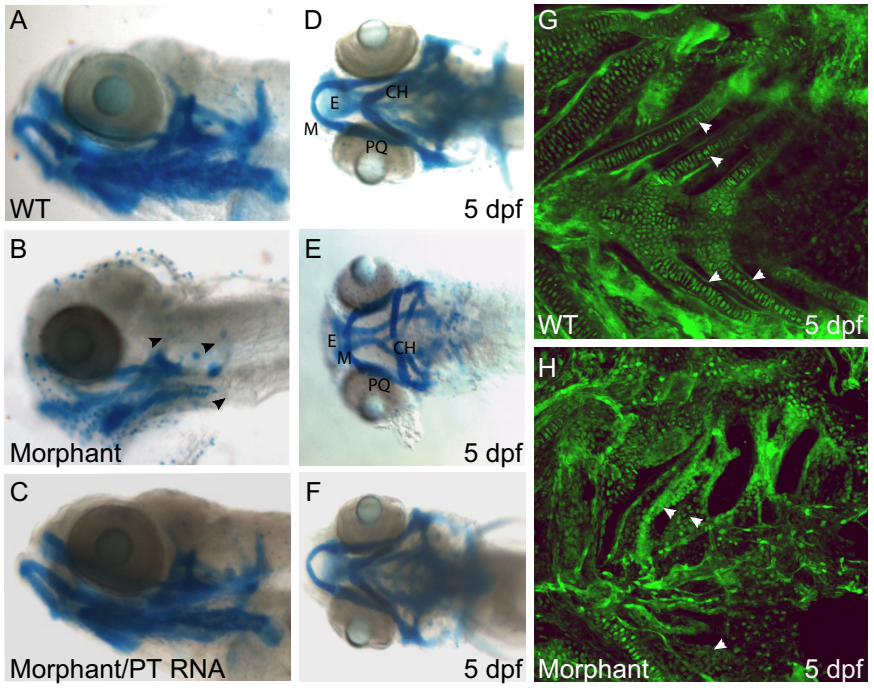

Figure 2. Phosphotransferase morphants display pronounced craniofacial defects. Alcian blue staining of wild-type (WT) (**A** and **D**) and morphant (**B** and **E**) embryos (5 dpf) revealed significant dysmorphogenesis of the jaw. Lateral views (**A–C**) highlight the protracted nature of the jaw, as well as the lack of Alcian blue positive auditory capsule structures (**B**, **arrowheads**), whereas ventral views (**D–F**) clearly demonstrate the reduction of morphant brachial rays and missing pectoral fins (**E**). Introduction of wild-type phosphotransferase mRNA resulted in complete rescue of these structural anomalies (**C** and **F**). Confocal analysis of *fli1*:EGFP embryos showed that, although the chondrocytes had condensed into distinct branchial rays by 5 dpf in wild-type (**G, white arrows**) embryos, morphant (**H**) embryos lacked mature cartilage elements in these regions. Interestingly, although the morphant cells were not differentiated into stacks of elongated chondrocytes, the branchial domains of phosphotransferase embryos were haphazardly populated with a large number of round GFP-positive cells (**H**, **white arrows**).

Table 1. Phosphotransferase Activity in Wild-Type and Morphant Embryos

MO injected	MO (ng)	% Knockdown	Phenotypes and % embryos affected
	0	0	None
TB	0.1	40	None
TB	0.5	58	M (15%)
TB	4.2	70	M, CF (100%); H (20%)
TB	8.2	89	M, CF, H (100%)
SB	8.2	86	M, CF, H (100%)
MM	8.2	<5	M, CF, H (<3%)

TB, translation-blocking MO; SB, splice-blocking MO; MM, 4-bp mismatch MO; M, motility defect, CF, craniofacial defects; H, pericardial edema.

Morphality is shown in nanogram.

To definitively establish that the phenotypes associated with MO injection were solely due to inhibition of phosphotransferase activity, we performed rescue experiments on morphants using wild-type zebrafish phosphotransferase mRNA. Sequential injection of the splice blocking MO and wild-type mRNA resulted in embryos that were indistinguishable from uninjected animals and animals injected with mRNA alone (data not shown; Figure 1, A and C). The rescued embryos swam and ate normally, lacked any obvious heart defects, and developed normal pectoral fins. In addition, these animals had normal swim bladders, well-developed eyes, and used their yolks within 5 to 6 days. Finally, the rescued embryos had elongated cranial structures and protruding jaws that resembled wild-type embryos (Figure 1, D and F). Taken together, these data suggest that the phenotypes observed following inhibition of phosphotransferase expression are specific to the loss of phosphotransferase activity.

Inhibition of Phosphotransferase Activity Resulted in Reduced Mannose Phosphorylation of Lysosomal Hydrolases

The phosphotransferase enzyme is responsible for initiating the biosynthesis of M6P residues on most lysosomal hydrolases. Thus, decreased enzyme activity is expected to result in loss of M6P residues on the oligosaccharides of lysosomal enzymes that use this targeting pathway. We next sought to determine the degree to which inhibition of phosphotransferase activity leads to a reduction in the mannose phosphorylation of such hydrolases. For these experiments, detergent extracts of wild-type and morphant embryos were passed over a cation-independent M6P receptor (CI-MPR) affinity column that binds to enzymes bearing M6P residues. After elution with 5 mmol/L M6P to recover M6P-modified lysosomal hydrolases, the activity of several hydrolases was measured in the column fractions, and the percentage of each enzyme that bound to the column and was selectively eluted with M6P was calculated (Table 2). As shown, in wild-type embryos, 17 to 23% of the total activity of three M6P-modified hydrolases bound to the column. In contrast, the bound enzyme activity was substantially reduced in morphant extracts (Table 2). These findings confirm that loss of phosphotransferase activity in the morphant embryos resulted in decreased mannose phosphorylation of lysosomal glycosidases.

Table 2. Mannose Phosphorylation of Lysosomal Hydrolases in Whole Wild-Type and Phosphotransferase Morphant Embryos

Lysosomal hydrolase	% of activity bound to the CI-MPR column	
	Wild type ($n = 3$)	Morphant ($n = 3$)
β-Galactosidase	18.4 ± 3.3	11.7 ± 1.9
β-Glucuronidase	17.5 ± 2.0	7.6 ± 1.5
β-Hexosaminidase	23.4 ± 3.1	9.6 ± 2.5

Detergent extracts from 4-day-old wild-type and morphant embryos were fractionated on the CI-MPR column, and bound activity relative to the total activity was determined.

Phosphotransferase Morphants Exhibit Reduced Motility

Inhibition of phosphotransferase activity led to a pronounced motility defect that was apparent by 24 hpf. At this time point, normal zebrafish embryos typically exhibit two different motility behaviors: spontaneous movements, consisting of slow alternating tail flexures, and elicited movements, where embryos respond to external stimuli with rapid tail flexures. Analysis of morphant embryos (at 24 hpf) revealed decreases in both of these behaviors. Whereas wild-type embryos spontaneously flex their tails frequently (19.8 ± 7.2 times/minute), morphant embryos rarely coiled their tails in the absence of mechanical stimulation (2.9 ± 2.6 times/minute). In addition, phosphotransferase-deficient embryos rarely exhibited the rapid side-to-side tail flexions characteristic of healthy embryos but were capable of limited movement following stimulation. The tail flexions of morphant embryos were uncoordinated, slower, and often restricted to one side of the body. Furthermore, wild-type clutch mates hatched from their chorions between 2 and 3 dpf, whereas the morphants generally required manual removal of the chorion and many were still unhatched by 5 dpf. Morphant embryos also displayed defects in later stage swimming behaviors. While wild-type embryos swam actively by the third day of development, the majority of morphant embryos (88 ± 5%) were typically found lying on their sides. Taken together, these data indicate that loss of phosphotransferase activity adversely affected multiple aspects of motor function.

Phosphotransferase Morphants Have Pronounced Craniofacial Defects

Because our initial phenotypic analysis of morphant embryos revealed rounded neurocraniums and protracted mouths, we investigated whether these phenotypes were associated with defects in the craniofacial development, a hallmark feature of ML-II. Analysis of embryos stained with Alcian blue at 3 (data not shown) and 5 dpf (Figure

2) revealed striking dysmorphogenesis of several cartilage elements in the morphants. The shapes of these elements and the angles of articulation between individual structures were consistently altered, particularly within portions of the jaw. In contrast to the elongated jaws of wild-type embryos (Figure 2, A and D), morphant jaws were shorter along the rostral-caudal axis but wider along the left-right axis (Figure 2, B and E). Morphometric measurements of cartilage structures demonstrated that Meckel's cartilages of morphant embryos were 7.5 ± 1.2% wider than wild-type cartilages along the short axis and 6 ± 1% shorter along their long axis. In wild-type embryos, Meckel's cartilage was typically positioned directly beneath the ethmoid plate, whereas this structure developed in a position posterior to the ethmoid plate in morphants (Figure 2, D and E). As a result, the associations among Meckel's cartilage, the palatoquadrate, and the ceratohyal bones (CH) were distorted, producing morphants with a broader, more flattened jaw. Introduction of wild-type phosphotransferase mRNA resulted in complete rescue of these structural anomalies (Figure 2, C and F).

Unlike the anterior structures (which although misshapen are present), posterior elements, including portions of the auditory capsule, the occipital arches, and the branchial rays, were either completely absent or significantly reduced in the phosphotransferase morphants (Figure 2, B and E, arrowheads). To determine whether these structures were indeed missing or whether the lack of Alcian blue staining simply reflected altered production of acidic matrix components, we generated morphant embryos in the Tg(*fli1*:EGFP)^{y1} transgenic background. The *fli1:EGFP* transgene labels a subset of neural crest (NC) cells, which ultimately give rise to craniofacial chondrocytes. Developing craniofacial structures can therefore be followed fluorescently in this line. MO knockdown of phosphotransferase activity in the *fli1*:EGFP background resulted in dysmorphic craniofacial structures identical to those observed in morphants of the other genetic strains tested. Analysis of *fli1*:EGFP-positive chondrocytes confirmed that mature forms of several of the posterior structures, including portions of the auditory capsule and the pharyngeal rays, had not developed in morphant embryos (Figure 2, G and H). We did, however, note some GFP-positive cells populating the presumptive domains of posterior cartilage formation. These morphant cells lacked the elongated shape and regular organization of wild-type chondrocytes (Figure 2G, arrowheads) and were instead small and round and highly disorganized (Figure 2H, arrowheads). Taken together, these data indicate that lack of morphant cartilages within the posterior regions may stem from alterations in the chondrocyte maturation program rather than a loss of the NC-derived progenitor cells.

Wild-Type and Morphant Animals Contain Similar Numbers of NC Cells during the First 2 Days of Development

To determine whether early aspects of NC cell development were altered, we first determined whether similar numbers of these cells were present in wild-type and morphant embryos. Wild-type and morphant *fli1*:EGFP embryos were dissociated into single-cell suspensions and subjected to FACS analysis (Table 3). At both 24 and 48 hpf, similar percentages of GFP-positive cells (relative to GFP-negative cells) were detected. Although these data suggested that wild-type and morphant embryos contained similar percentages of GFP-positive NC cells, we could not rule out the possibility that differences in the distribution of NC cells did exist. Because the *fli1*:EGFP transgene is active in cell lineages other than those derived from the NC, it was also possible that subtle differences in the number of NC cells might be masked by other GFP-positive populations. In light of this possibility, we performed *in situ* hybridization of sox9b, a known marker of pre- and postmigratory NC cells (Figure 3A). This analysis showed no obvious differences in either the intensity or pattern of sox9b-positive cells between 11 and 14 hpf, suggesting that phosphotransferase activity is not essential for the earliest aspects of premigratory NC cell development. Sox9b in situs of embryos 17–20 hpf was also similar. Although sox9b expression had been down-regulated across the majority of cranial field by 17 hpf, both wild-type and morphant embryos maintained strong expression within the pectoral fin buds. In addition, both wild-type and morphant embryos showed prominent sox9b expression across the anterior forebrain and nasal cavity at 20 hpf. We did not detect any differences in the expression of the sox9a transcript at these time points (data not shown). Interestingly, however, several regions were noted within morphant embryos that lacked normal sox9b expression. These included four distinct stripes of sox9b-positive cells normally present caudal to the otic vesicle. Collectively, these data demonstrated that, although inhibition of phosphotransferase activity does not appear to significantly alter the number or distribution of premigratory NC cells, it could affect a subset of NC once the cells become mobile.

Table 3. FACS Analysis of GFP-Positive Cells

Age		% GFP negative	% GFP positive
1 Day			
	Wild type	95.0	5.0 ± 0.6
	Morphant	94.8	5.2 ± 0.4
2 Day			
	Wild type	95.4	4.6 ± 0.6
	Morphant	94.7	5.1 ± 1.1
3 Day			
	Wild type	77.2	22.8 ± 2.0
	Morphant	72.6	27.4 ± 1.4

Loss of Phosphotransferase Activity Does Not Alter the Proliferation or Cell Fate Specification of Prechondrocytic Cells in the Pharyngeal Pouches

We next sought to address whether other aspects of early chondrocyte development were affected in the morphants, focusing on postmigratory events such as pro-

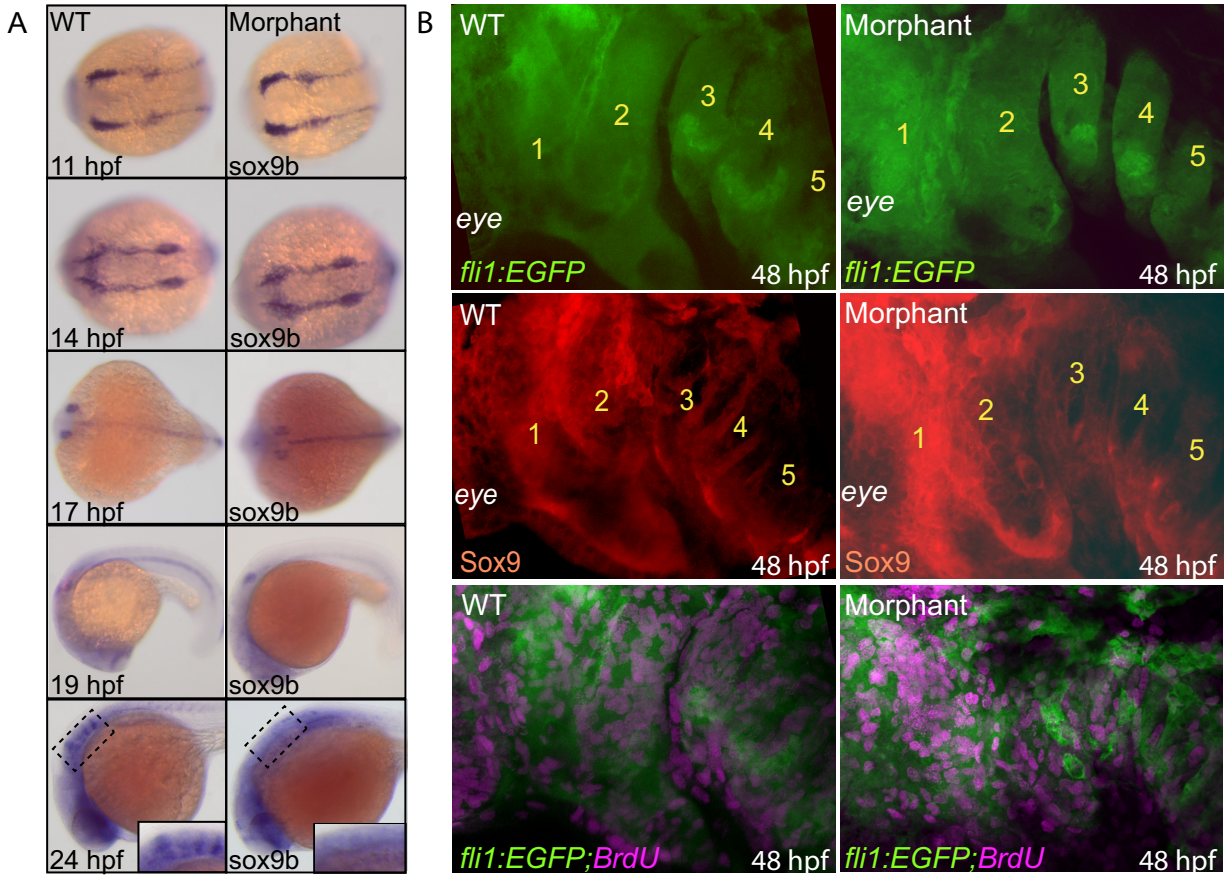

Figure 3. Early aspects of NC development appear normal. **A:** *In situ* analysis of sox9b expression in wild-type (WT) and morphant embryos show no obvious differences between 11 and 19 hpf. By 24 hpf, several sox9b-positive stripes were notably absent from morphant embryos (see **boxed region** and **inset**). **B:** Confocal analysis of wild-type and morphant *fli1*:EGFP embryos show that both have strong EGFP-positive fluorescence throughout the pharyngeal arches (numbered in yellow 1 to 5). In both cases, immunohistochemical staining for Sox9 (red) also showed strong staining in the same regions. Immunohistochemical stains of BrdU-labeled (purple) embryos demonstrated similar indexes of proliferation throughout these regions.

liferation and cell fate specification of the NC-derived chondroctye precursors present in the pharyngeal arches. As shown in Figure 3B, confocal imaging of *fli1*:EGFP embryos revealed that the pharyngeal regions of both wild-type and morphant animals were highly positive for GFP, indicating that *fli1*-positive cells were capable of migration into and expansion within these regions. Confocal analysis of BrdU-labeled embryos also demonstrated that the GFP-positive cells within the pharyngeal arches proliferated at similar rates in wild-type and morphant embryos (18 ± 4% of the GFP-positive cells in wild-type samples were also BrdU positive, compared with 20 ± 5% of morphant cells staining positive for both GFP and BrdU). FACS analyses of cells isolated from *fli1*:EGFP embryos at 72 hpf detected no significant differences in the number of GFP-positive cells between wild-type (22.8 ± 2%) and morphant (27.4 ± 1.4%) embryos (Table 3). These data suggest that, although alterations in migratory patterns and proliferation indexes of subsets of NC cells may exist, the majority of cells that contribute to anterior cartilage development do ultimately populate the arches and expand at similar rates.

We next addressed whether the *fli1*:EGFP-positive cells populating the pharyngeal arches continued to express sox9, which not only serves as a marker for early NC but also functions to specify the fate of early chondroctyes. Whole-mount immunohistochemical analyses of 48-hour-old animals showed that the GFP-positive cranial NC cells within the arches of wild-type and morphant embryos expressed sox9 in a spatially and temporally similar manner. Normal expression of sox9 in the anterior arches of the morphants suggests that the NC cells in the arches are committed to the chondrocyte cell fate. These data support the conclusion that the primary defect leading to dysmorphogenesis of the anterior structures occurs after the NC cells reach the pharyngeal arches.

The Craniofacial Defects in the Morphants Is Associated with Striking Alterations in the Expression of Type II Collagen

To analyze the effect of impaired M6P biosynthesis on the late-stage aspects of NC cell development, we examined several parameters of chondrocyte condensation and differentiation (Figure 4). Once in the pharyngeal arches, specific domains of chondrocytes condense to form the primordia of spatially defined craniofacial structures. This condensation is followed by multiple phases of differentiation, whereby NC cells commit to the chondrocyte

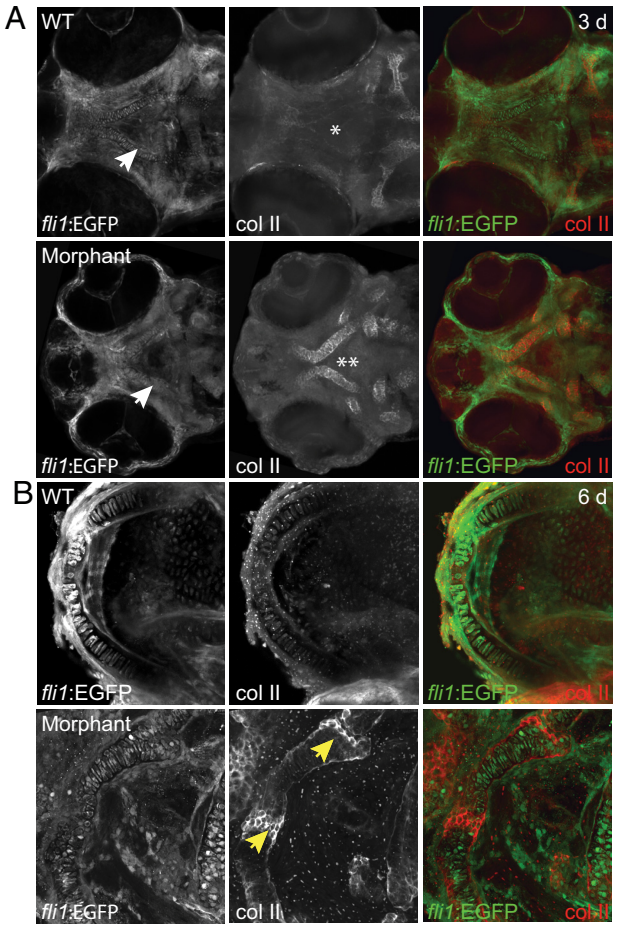

Figure 4. Inhibition of phosphotransferase activity results in disruptions in type II collagen expression. Wild-type (WT) and morphant embryos were stained immunohistochemically for type II collagen. **A:** Although condensing chondrocytes were visible by *fli1*:EGFP expression in both wild-type and morphant embryos at 3 dpf (**white arrows**), very little type II collagen expression was detected in wild-type anterior cartilages (**asterisk**), such as the trabeculum. Conversely, morphant trabecular chondrocytes expressed significantly higher levels of collagen (**double asterisk**). **B:** By 6dpf, collagen expression remained elevated. This was particularly evident within the articulations between individual cartilages of the morphant jaw (**yellow arrows**).

cellular fate. As craniofacial chondrocytes differentiate, they wrap themselves in a collagen-based ECM, reorganize through morphogenetic movements, become hypertrophic, and undergo apoptosis and mineralization. A comparison of wild-type and morphant embryos at 3 dpf revealed striking differences in several aspects of this differentiation program. First, the timing and localization of collagen deposition is altered in morphant embryos, as assayed by immunohistochemical staining for type II collagen—one of the earliest markers of chondrocyte differentiation. Morphant embryos expressed high levels of type II collagen that was only detectable at low levels in wild-type embryos (Figure 4A). This trend continued at 6 dpf, with morphant jaws and neurocraniums containing significantly more type II collagen than their wild-type clutch mates. The presence of type II collagen was particularly evident within the articular regions between cartilage elements of the jaw (Figure 4B). A corresponding elevation (20-fold) in type II collagen transcript abundance was also observed by quantitative PCR analyses of extracts generated from the heads of wild-type and morphant embryos (data not shown). Although many of the cells within wild-type cartilages had reorganized to form a single row of tightly packed cells by 3 dpf, the majority of the cells within morphant structures were under intercalated (Figure 5, A–E). This defect was evident in both high power confocal images and low power electron micrographs. Third, morphant chondrocytes were 25 ± 2% larger than wild-type counterparts, suggesting that morphant embryos may have experienced an early onset of cellular hypertrophy (Figure 5F). It is also possible that the increased size of morphant chondrocytes indicates the storage of undigested cellular material. However, we were unable to detect any obvious signs of lysosomal storage in tissues by staining with periodic acid-Schiff or Lysotracker.

Sox9 Is Inappropriately Expressed in the Condensing Chondrocytes of Morphant Embryos

In addition to its role in specifying NC cells, Sox9 is required for multiple aspects of chondrocyte differentiation, including expression of type II collagen.[34–37] Confocal analyses of Sox9-stained embryos revealed that, although the GFP-positive chondrocytic cells of the wild-type neurocraniums had begun to condense into the trabecular cartilage at 48 hpf (Figure 6A, yellow arrows), they did not yet express the Sox9 protein. Furthermore, wild-type embryos demonstrated a clear demarcation of Sox9 expression that was excluded from the chondrocyte boundary (Figure 6, A, white dashed line, and B). In contrast, the morphant chondrocytes, which were also condensing to form the trabecular cartilage, had inappropriately begun to express high levels of Sox9 protein. In fact, the boundary of Sox9 expression in the morphants was not only expanded to include the chondrocytes but also significantly disrupted in the more posterior portion of the cranial field (Figure 6, A, yellow asterisks, and B). The inappropriate expression of Sox9 within morphant chondrocytes supports the notion that alterations in aspects of the chondrocyte differentiation program contribute to the cartilage malformations observed in morphants.

Altered Otolith Formation in the Phosphotransferase Morphants

On the basis of the findings above, it was not clear whether loss of phosphotransferase activity had caused the NC cells to both enter and complete their differentiation program early, or whether the morphant cells had simply upregulated the expression of sox9 and type II collagen but not actually induced the full differentiation program. To address this issue, wild-type and morphant embryos were dually stained with Alcian blue and Alizarin red, a dye that complexes with deposited calcium. Analysis of wild-type and morphant craniofacial cartilages did not reveal any obvious differences in the degree of Aliza-

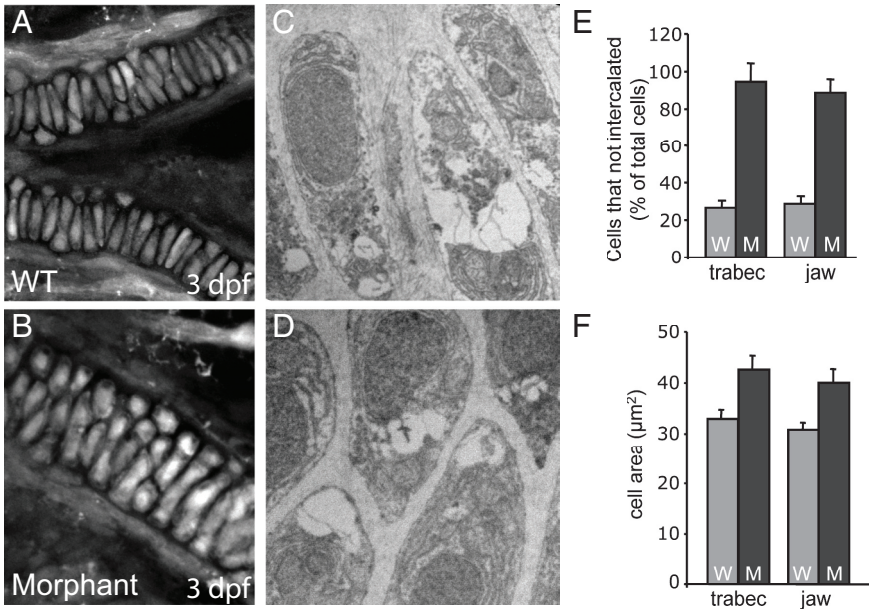

Figure 5. Morphant chondrocytes both failed to intercalate and were larger than wild-type (WT) cells. High-power confocal analysis (**A** and **B**) and electron micrographs (**C** and **D**) of *fli1*:EGFP embryos revealed that, although wild-type cartilages were one cell wide (**A** and **C**), morphant chondrocytes had failed to intercalate and were therefore often several cells in diameter (**B** and **D**). This was evident throughout portions of both the trabeculum and the jaw (as quantitated in **E**). In addition, morphant chondrocytes were 25% larger than wild-type cells within these same regions (**F**).

rin red-positive staining (Figure 7, A–D). However, we did note striking changes in both the structure and the mineralization of the morphant otic vesicles. The otic vesicles of morphant embryos were smaller in size, irregularly shaped and exhibited clear differences in the pattern and intensity of Alizarin red staining. In particular, morphant stones lacked any internal mineralized fibers.

Smad2 Phosphorylation Is Increased in the Otic Vesicles of Morphant Embryos

Several recent lines of evidence have suggested that downstream effectors of the TGF-β pathway (eg, Smad2/3) cooperate with sox9 to induce expression of type II collagen in developing cranial cartilages.[37] To assess whether the alterations in type II collagen and sox9 also correlated with changes in TGF-β signaling, whole wild-type and morphant embryos were stained with an antibody that recognizes phosphorylated forms of Smad2 (Figure 8). These experiments demonstrated several differences in the overall pattern of Smad2 phosphorylation within the heads of wild-type and morphant embryos. In particular, the region of Smad2 phosphorylation was expanded within the anterior regions, whereas the posterior regions appeared to express more restricted domains of phosphorylated Smad2. Interestingly, we also

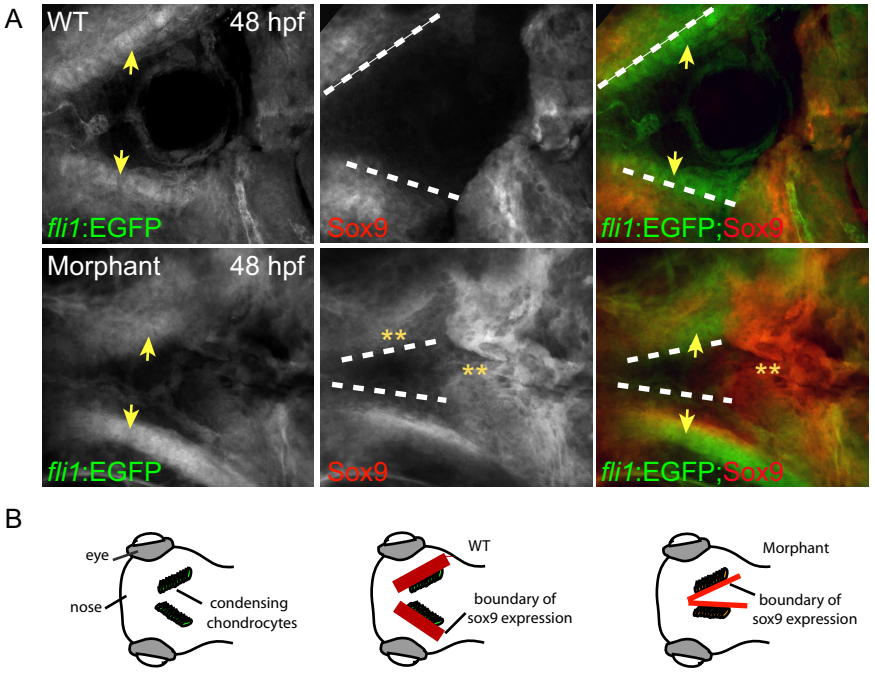

Figure 6. Sox9 is abnormally expressed within the developing cartilage of phosphotransferase morphants. **A:** Immunohistochemical staining of Sox9, a transcriptional regulator of chondrocyte differentiation, revealed that, although wild-type (WT) chondrocytes lacked any detectable expression at 2 dpf, morphant cells contained high levels both within the chondrocytes themselves as well as throughout the cranial region. **Yellow arrows** denote the location of condensing chondrocytes. **Dashed white lines** mark the boundaries of Sox9 expression in the anterior head. Analysis of these boundaries in merged images of *fli1*:EGFP and Sox9 expression demonstrates that in wild-type embryos Sox9 expression does not overlap with *fli1*:EGFP-positive chondrocytes. In contrast, Sox9 is highly expressed in morphant chondrocytes. Although these images represent maximal intensity projections of several confocal planes, the presence of Sox9 expression was confirmed within individual planes as well (data not shown). **Yellow asterisks** highlight regions where Sox9 is inappropriately expressed in morphant embryos. **B:** Schematic representation of condensing chondrocytes and the associated pattern of Sox9 expression in wild-type and morphant embryos.

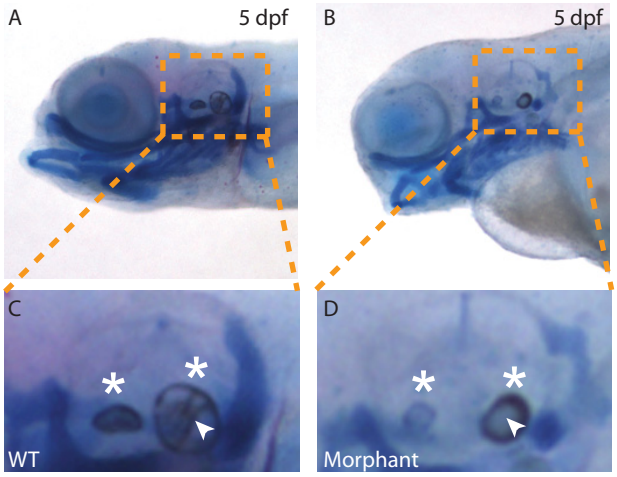

Figure 7. Otic vesicle development is altered in phosphotransferse morphants. Wild-type (WT) (**A** and **C**) and morphant (**B** and **D**) embryos were dually stained with Alcian blue and Alizarin red. Magnified views of the **yellow boxes** (**C** and **D**) of the otic vesicles highlight several striking differences in the size, shape, and nature of the ear stones (otiliths, **white asterisks**) in morphant embryos. Of particular note are disruptions in the mineralization pattern of the rims of morphant otiliths (as detected by Alizarin red staining) as well as the complete lack of a mineralized internal matrix (**white arrowheads**).

noted dramatic increases in the amount of phosphorylated Smad2 within the otic vesicles of morphant embryos. Strong Smad2 staining was primarily associated with the morphant otiliths. Taken together, these findings indicate that changes in downstream effectors of the TGF-β pathway accompany the otic vesicle phenotypes.

Discussion

The molecular mechanisms that underlie the developmental defects associated with ML-II and related LSDs remain poorly defined. Gaining insight into the disease process is critical, however, because it may inform new ways to treat this disorder without having to overcome the current challenges of replacing the defective enzyme or gene. Investigating the pathogenesis of ML-II has been particularly hampered by the lack of animal models that are both genetically accessible and amenable to the study of early developmental processes. In this article, we demonstrate that loss of phosphotransferase activity (the defective enzyme in ML-II) in zebrafish embryos results in multiple defects, including impaired cartilage development and motility as well as altered otic vesicle formation. Importantly, many of the affected systems in the phosphotransferase-deficient embryos, including craniofacial cartilage, also develop abnormally in human ML-II patients. Using this model, we uncovered striking alterations in the timing and expression of chondrogenic factors (eg, type II collagen and Sox9) in developing cartilage structures as well as abnormal matrix formation and calcium deposition in morphant otoliths. Collectively, these data suggest that impaired production and/or maintenance of ECM proteins are integral to the development of these phenotypes.

Because phosphotransferase is the only known enzyme responsible for initiating M6P biosynthesis, a reduction in its expression and activity should result in loss of these recognition markers on lysosomal hydrolases. Fractionation of detergent extracts of phosphotransferase morphants using a M6P receptor affinity column did in fact show a significant decrease in the activity of three different hydrolases recovered from this column (Table 2). On the basis of the robust knockdown of phosphotransferase enzyme activity in the morphants, we were surprised to find such a sizable proportion of enzyme activity bound to the CI-MPR column in these embryos. It is possible, however, that this fraction of activity represents M6P-modified lysosomal hydrolases that are stored within the yolk of the embryos (and thus not sensitive to the translation or splice-blocking MOs). Indeed, we detected a large amount of M6P-modified β-galactosidase activity present in zebrafish eggs. However, it is unclear at this time where this yolk-deposited enzyme is predom-

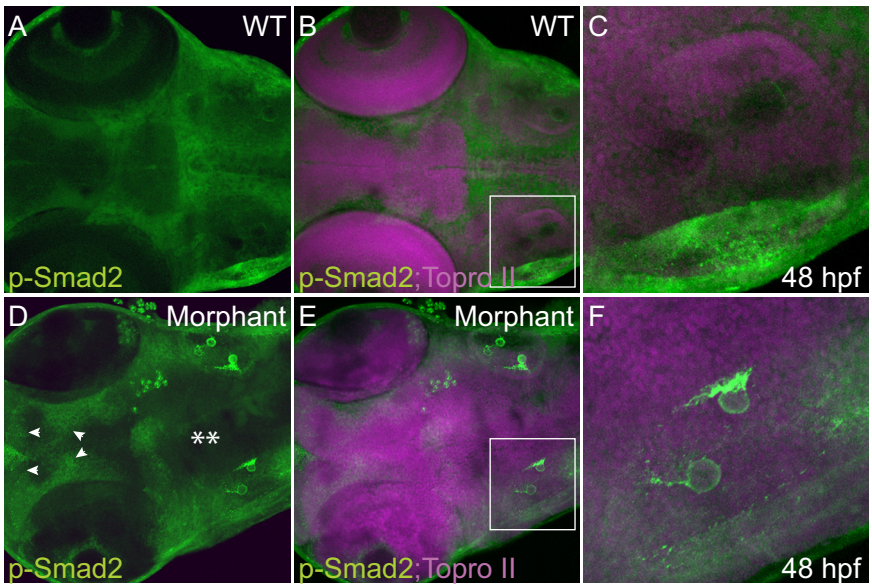

Figure 8. Smad2-dependent TGF-β signaling is altered in regions of phosphotransferase morphants. Wild-type (WT) (**A–C**) and morphant (**D–F**) embryos were stained immunohistochemically at 2 dpf for phopshorylated forms of Smad2. Confocal analysis of these animals revealed several changes in the pattern of Smad2 phosphorylation (as denoted by **white arrowheads** and **asterisks**). Smad2 phosphorylation was particularly high in the otiliths of the morphant otic vesicles (**E** and **F**) compared with wild-type otiliths (**B** and **C**). **C** and **F** represent magnified views of boxed regions from **B** and **E**. Nuclei are a stained with Topro II (purple, **B**, **C**, **E**, and **F**).

inantly found throughout the embryo or whether it can reach and be taken up by the developing tissues, in particular craniofacial cartilage. A thorough analysis of the level of mannose phosphorylation of lysosomal glycosidases and proteases in zebrafish is ongoing and should yield information regarding potential proteins involved in the development of the phenotypes associated with this model.

The analyses of Alcian blue-stained cartilage structures in wild-type and morphant embryos revealed numerous phenotypes that ranged in severity from distortions in shape (anterior elements) to complete loss of mature cartilage structures (pectoral fins and portions of the auditory capsule). These phenotypes were associated with strong and persistent increases in the expression of type II collagen as judged by immunohistochemical staining and quantitative PCR analysis. These data in conjunction with noted alterations in the timing and localization of Sox9 expression indicate that loss of phosphotransferase activity adversely affects the chondrocyte differentiation program. This is further supported by the fact that morphant chondrocytes both failed to properly intercalate and were significantly larger than wild-type cells. Although it is not clear why the posterior structures are more severely affected than anterior elements, the robust nature of these phenotypes may reflect an increased requirement for phosphotransferase activity and lysosomal function in these regions. Conversely, the graded nature of the phenotypes along the rostral to caudal axis may reflect local disruptions in the activity of one or more growth factors required for different aspects of chondrogenesis.

It is well established that members of the TGF-β superfamily play a critical role during several aspects of chondrocyte differentiation.[38–42] This is evidenced by the fact that dysregulation of TGF-β signaling, at the level of the ligand or receptor, is associated with craniofacial and skeletal abnormalities in humans. Although many signaling pathways may be disrupted following inhibition of phosphotransferase activity, we believe that the involvement of TGF-βs is likely for several reasons. First, several TGF-βs have been shown to regulate cartilage development through their ability to control the expression and deposition of ECM proteins in chondrocyte precursors. In particular, expression of type II collagen is regulated in developing cartilage by the cooperative activity of Sox9 and TGF-β-dependent Smad2/3 signals.[37,43,44] Immunohistochemical analysis of wild-type and phosphotransferase morphant embryos showed that the expression patterns of both Sox9 and phosphorylated forms of Smad2 were altered throughout the craniofacial region. Second, several members of the TGF-β family are known to interact with specific components of the ECM, which in turn provides a mechanism for regulating their bioavailability and local activities. Thus, disruptions in the composition of the matrix can significantly alter the timing and localization of TGF-β activity. In addition to our data regarding type II collagen expression, we observed changes in the deposition and expression profiles of fibronectin and laminin (data not shown), as well as Alizarin red-positive mineralization. It is intriguing to speculate that changes in the integrity of the ECM, perhaps due to the mislocalization or inappropriate activity of lysosomal proteases, can result in disruptions in the timing of key growth factor signaling pathways.

In addition to the early expression of type II collagen within the trabecular chondrocytes of phosphotransferase morphants, we noted an apparent accumulation of this ECM protein at later stages of development, in particular within the articulations of jaw elements (Figure 4B). This accumulation may represent sustained overexpression of type II collagen (consistent with an altered differentiation program). Indeed, type II collagen overexpression has been noted in several tissues from patients with mucopolysaccharidoses.[45,46] This observation could also reflect impaired clearance of type II collagen within the intercalating chondrocytes. The turnover of collagen within developing bone and cartilage begins with its initial proteolysis within the pericellular space by a group of secreted or membrane-associated matrix metalloproteinases.[47,48] Complete turnover may either be completed outside the cell by the action of gelatinases such as metalloproteinase-2 or following endocytosis of defined fragments into the cell, transport to lysosomes, and proteolytic degradation of acid-denatured collagen by cathepsins. Loss of the cathepsin proteases from the lysosomes, a common feature in some ML-II cell types, may therefore result in failure to fully degrade type II collagen and other ECM proteins via the intracellular pathway. Alternatively, enhanced secretion and activity of these proteases because of loss of the M6P recognition markers might affect the stability and turnover of matrix components, including cartilage proteoglycans and collagens. Regardless, one would predict that impaired clearance or persistent expression of type II collagen could impact normal development and morphogenetic movement of chondrocytes by altering the ability of these cells to either properly navigate within their environment or change their shape during the intercalation process.

Our data suggest that the development of structures highly dependent on the coordinated biosynthesis and remodeling of ECM proteins (ie, cartilage and otoliths) appear to be uniquely sensitive to the loss of phosphotransferase activity and M6P biosynthesis. These observations are consistent with the early observations in bone and cartilage samples from postmortem ML-II patients.[19,49] In light of these findings, we have begun to address whether additional phenotypes in the morphant embryos such as impaired motility and abnormal eye development may also involve ECM-derived defects. Such a possibility is supported by recent evidence demonstrating a critical role for the biosynthesis of ECM proteins, such as collagen XVIII and fibronectin, in the establishment of neuromuscular development and motility in zebrafish.[50,51]

Taken together, our results provide new cellular and molecular insight into the craniofacial defects associated with ML-II and establish the utility of the zebrafish system in the investigation of LSDs. The further characterization of this model and the development of zebrafish that model other related lysosomal disorders will provide an

excellent opportunity to explore the developmental impact of impaired lysosomal function. Such models will also provide an ideal platform for the assessment of new therapeutic strategies.

Acknowledgments

We acknowledge Dr. Peter Lobel for his gift of the CI-MPR affinity column and Dr. William Canfield for providing the [^{32}P]UDP-GlcNAc used in the phosphotransferase assays. We also thank Drs. John Postlethwait and Nathan Lawson for providing key reagents and Mary Ard for assistance with electron microscopy. We are very grateful to both Dr. Stuart Kornfeld and Dr. Rachel Wong for their early support of this work.

References

1. Futerman AH, van Meer G: The cell biology of lysosomal storage disorders. Nat Rev Mol Cell Biol 2004, 5:554–565
2. Kornfeld S, Mellman I: The biogenesis of lysosomes. Annu Rev Cell Biol 1989, 5:483–525
3. von Figura K: Molecular recognition and targeting of lysosomal proteins. Curr Opin Cell Biol 1991, 3:642–646
4. Ghosh P, Dahms NM, Kornfeld S: Mannose 6-phosphate receptors: new twists in the tale. Nat Rev Mol Cell Biol 2003, 4:202–212
5. Bao M, Booth JL, Elmendorf BJ, Canfield WM: Bovine UDP-*N*-acetylglucosamine:lysosomal-enzyme *N*-acetylglucosamine-1-phosphotransferase. I. Purification and subunit structure. J Biol Chem 1996, 271:31437–31445
6. Bao M, Elmendorf BJ, Booth JL, Drake RR, Canfield WM: Bovine UDP-*N*-acetylglucosamine:lysosomal-enzyme *N*-acetylglucosamine-1-phosphotransferase. II. Enzymatic characterization and identification of the catalytic subunit. J Biol Chem 1996, 271:31446–31451
7. Kudo M, Bao M, D'Souza A, Ying F, Pan H, Roe BA, Canfield WM: The α and β subunits of the human UDP-*N*-acetylglucosamine:lysosomal enzyme *N*-acetylglucosamine-1-phosphotransferase [corrected] are encoded by a single cDNA. J Biol Chem 2005, 280:36141–36149
8. Lee WS, Payne BJ, Gelfman CM, Vogel P, Kornfeld S: Murine UDP-GlcNAc:lysosomal enzyme *N*-acetylglucosamine-1-phosphotransferase lacking the γ subunit retains substantial activity toward acid hydrolases. J Biol Chem 2007, 282:27198–27203
9. Kornfeld R, Bao M, Brewer K, Noll C, Canfield W: Molecular cloning and functional expression of two splice forms of human *N*-acetylglucosamine-1-phosphodiester α-*N*-acetylglucosaminidase. J Biol Chem 1999, 274:32778–32785
10. Kornfeld R, Bao M, Brewer K, Noll C, Canfield WM: Purification and multimeric structure of bovine *N*-acetylglucosamine-1-phosphodiester α-*N*-acetylglucosaminidase. J Biol Chem 1998, 273:23203–23210
11. Kudo M, Brem MS, Canfield WM: Mucolipidosis II (I-cell disease) and mucolipidosis IIIA (classical pseudo-hurler polydystrophy) are caused by mutations in the GlcNAc-phosphotransferase α/β subunits precursor gene. Am J Hum Genet 2006, 78:451–463
12. Bargal R, Zeigler M, Abu-Libdeh B, Zuri V, Mandel H, Ben Neriah Z, Stewart F, Elcioglu N, Hindi T, Le Merrer M, Bach G, Raas-Rothschild A: When mucolipidosis III meets mucolipidosis II: gNPTA gene mutations in 24 patients. Mol Genet Metab 2006, 88:359–363
13. Steet RA, Hullin R, Kudo M, Martinelli M, Bosshard NU, Schaffner T, Kornfeld S, Steinmann B: A splicing mutation in the α/β GlcNAc-1-phosphotransferase gene results in an adult onset form of mucolipidosis III associated with sensory neuropathy and cardiomyopathy. Am J Med Genet A 2005, 132:369–375
14. Tiede S, Cantz M, Spranger J, Braulke T: Missense mutation in the *N*-acetylglucosamine-1-phosphotransferase gene (GNPTA) in a patient with mucolipidosis II induces changes in the size and cellular distribution of GNPTG. Hum Mutat 2006, 27:830–831
15. Tiede S, Storch S, Lubke T, Henrissat B, Bargal R, Raas-Rothschild A, Braulke T: Mucolipidosis II is caused by mutations in GNPTA encoding the α/β GlcNAc-1-phosphotransferase. Nat Med 2005, 11:1109–1112
16. Kornfeld S: Trafficking of lysosomal enzymes in normal and disease states. J Clin Invest 1986, 77:1–6
17. Walkley SU: Pathogenic mechanisms in lysosomal disease: a reappraisal of the role of the lysosome. Acta Paediatr Suppl 2007, 96:26–32
18. Babcock DS, Bove KE, Hug G, Dignan PS, Soukup S, Warren NS: Fetal mucolipidosis II (I-cell disease): radiologic and pathologic correlation. Pediatr Radiol 1986, 16:32–39
19. Nogami H, Oohira A, Suzuki F, Tsuda K: Cartilage of I-cell disease. Pediatr Res 1981, 15:330–334
20. Aula P, Rapola J, Autio S, Raivio K, Karjalainen O: Prenatal diagnosis and fetal pathology of I-cell disease (mucolipidosis type II). J Pediatr 1975, 87:221–226
21. Mazrier H, Van Hoeven M, Wang P, Knox VW, Aguirre GD, Holt E, Wiemelt SP, Sleeper MM, Hubler M, Haskins ME, Giger U: Inheritance, biochemical abnormalities, and clinical features of feline mucolipidosis II: the first animal model of human I-cell disease. J Hered 2003, 94:363–373
22. Bosshard NU, Hubler M, Arnold S, Briner J, Spycher MA, Sommerlade HJ, von Figura K, Gitzelmann R: Spontaneous mucolipidosis in a cat: an animal model of human I-cell disease. Vet Pathol 1996, 33:1–13
23. Hubler M, Haskins ME, Arnold S, Kaser-Hotz B, Bosshard NU, Briner J, Spycher MA, Gitzelmann R, Sommerlade HJ, von Figura K: Mucolipidosis type II in a domestic shorthair cat. J Small Anim Pract 1996, 37:435–441
24. Gelfman CM, Vogel P, Issa TM, Turner CA, Lee WS, Kornfeld S, Rice DS: Mice lacking α/β subunits of GlcNAc-1-phosphotransferase exhibit growth retardation, retinal degeneration, and secretory cell lesions. Invest Ophthalmol Vis Sci 2007, 48:5221–5228
25. Vogel P, Payne B, Read R, Lee WS, Gelfman C, Kornfeld S: Comparative pathology of murine mucolipidosis types II and IIIC. Vet Pathol 2009, 46:313–324
26. Kimmel CB, Ballard WW, Kimmel SR, Ullmann B, Schilling TF: Stages of embryonic development of the zebrafish. Dev Dyn 1995, 203:253–310
27. Lawson ND, Weinstein BM: In vivo imaging of embryonic vascular development using transgenic zebrafish. Dev Biol 2002, 248:307–318
28. Javidan Y, Schilling TF: Development of cartilage and bone. Methods Cell Biol 2004, 76:415–436
29. Walker M, Kimmel C: A two-color acid-free cartilage and bone stain for zebrafish larvae. Biotech Histochem 2007, 82:23–28
30. Harris JA, Cheng AG, Cunningham LL, MacDonald G, Raible DW, Rubel EW: Neomycin-induced hair cell death and rapid regeneration in the lateral line of zebrafish (Danio rerio). J Assoc Res Otolaryngol 2003, 4:219–234
31. Thisse C, Thisse B, Schilling TF, Postlethwait JH: Structure of the zebrafish snail1 gene and its expression in wild-type, spadetail and no tail mutant embryos. Development 1993, 119:1203–1215
32. Flanagan-Steet H, Fox MA, Meyer D, Sanes JR: Neuromuscular synapses can form in vivo by incorporation of initially aneural postsynaptic specializations. Development 2005, 132:4471–4481
33. Robu ME, Larson JD, Nasevicius A, Beiraghi S, Brenner C, Farber SA, Ekker SC: p53 activation by knockdown technologies. PLoS Genet 2007, 3:e78
34. Bell DM, Leung KK, Wheatley SC, Ng LJ, Zhou S, Ling KW, Sham MH, Koopman P, Tam PP, Cheah KS: SOX9 directly regulates the type-II collagen gene. Nat Genet 1997, 16:174–178
35. Lefebvre V, de Crombrugghe B: Toward understanding SOX9 function in chondrocyte differentiation. Matrix Biol 1998, 16:529–540
36. Yan YL, Miller CT, Nissen RM, Singer A, Liu D, Kirn A, Draper B, Willoughby J, Morcos PA, Amsterdam A, Chung BC, Westerfield M, Haffter P, Hopkins N, Kimmel C, Postlethwait JH: A zebrafish sox9 gene required for cartilage morphogenesis. Development 2002, 129:5065–5079
37. Furumatsu T, Tsuda M, Taniguchi N, Tajima Y, Asahara H: Smad3 induces chondrogenesis through the activation of SOX9 via CREB-binding protein/p300 recruitment. J Biol Chem 2005, 280:8343–8350
38. Janssens K, ten Dijke P, Janssens S, Van Hul W: Transforming growth factor-β1 to the bone. Endocr Rev 2005, 26:743–774
39. Kaartinen V, Voncken JW, Shuler C, Warburton D, Bu D, Heisterkamp N, Groffen J: Abnormal lung development and cleft palate in mice

lacking TGF-β3 indicates defects of epithelial-mesenchymal interaction. Nat Genet 1995, 11:415–421
40. Kinoshita A, Saito T, Tomita H, Makita Y, Yoshida K, Ghadami M, Yamada K, Kondo S, Ikegawa S, Nishimura G, Fukushima Y, Nakagomi T, Saito H, Sugimoto T, Kamegaya M, Hisa K, Murray JC, Taniguchi N, Niikawa N, Yoshiura K: Domain-specific mutations in TGF-β1 result in Camurati-Engelmann disease. Nat Genet 2000, 26:19–20
41. Taya Y, O'Kane S, Ferguson MW: Pathogenesis of cleft palate in TGF-β3 knockout mice. Development 1999, 126:3869–3879
42. Yang X, Chen L, Xu X, Li C, Huang C, Deng CX: TGF-β/Smad3 signals repress chondrocyte hypertrophic differentiation and are required for maintaining articular cartilage. J Cell Biol 2001, 153:35–46
43. Bi W, Deng JM, Zhang Z, Behringer RR, de Crombrugghe B: Sox9 is required for cartilage formation. Nat Genet 1999, 22:85–89
44. Healy C, Uwanogho D, Sharpe PT: Regulation and role of Sox9 in cartilage formation. Dev Dyn 1999, 215:69–78
45. Renteria VG, Ferrans VJ: Intracellular collagen fibrils in cardiac valves of patients with the Hurler syndrome. Lab Invest 1976, 34:263–272
46. De Franceschi L, Roseti L, Desando G, Facchini A, Grigolo B: A molecular and histological characterization of cartilage from patients with Morquio syndrome. Osteoarthritis Cartilage 2007, 15:1311–1317
47. Holmbeck K, Szabova L: Aspects of extracellular matrix remodeling in development and disease. Birth Defects Res C Embryo Today 2006, 78:11–23
48. Wagenaar-Miller RA, Engelholm LH, Gavard J, Yamada SS, Gutkind JS, Behrendt N, Bugge TH, Holmbeck K: Complementary roles of intracellular and pericellular collagen degradation pathways in vivo. Mol Cell Biol 2007, 27:6309–6322
49. Martin JJ, Leroy JG, Farriaux JP, Fontaine G, Desnick RJ, Cabello A: I-cell disease (mucolipidosis II):a report on its pathology. Acta Neuropathol 1975, 33:285–305
50. Schneider VA, Granato M: The myotomal diwanka (lh3) glycosyltransferase and type XVIII collagen are critical for motor growth cone migration. Neuron 2006, 50:683–695
51. Snow CJ, Peterson MT, Khalil A, Henry CA: Muscle development is disrupted in zebrafish embryos deficient for fibronectin. Dev Dyn 2008, 237:2542–2553